Molecular Immunology 48 (2011) 1245–1252

Contents lists available at ScienceDirect

Molecular Immunology

journal homepage: www.elsevier.com/locate/molimm

Characterization of a unique conformational epitope on free immunoglobulin kappa light chains that is recognized by an antibody with therapeutic potential

Andrew T. Hutchinson[a,b,*,1], Ralitza Alexova[a,1], Vanessa Bockhorni[a,1], Paul A. Ramsland[c,d,e], Darren R. Jones[a], Cameron V. Jennings[a], Kevin Broady[a,b], Allen B. Edmundson[f], Robert L. Raison[a,b]

[a] School of Medical and Molecular Biosciences, University of Technology Sydney, Ultimo, NSW 2007, Australia
[b] The iThree Institute, University of Technology Sydney, Ultimo, NSW 2007, Australia
[c] Centre for Immunology, Burnet Institute, Melbourne, VIC 3004, Australia
[d] Department of Immunology, Monash University, Alfred Medical Research and Education Precinct, Melbourne, VIC 3004, Australia
[e] Department of Surgery Austin Health, The University of Melbourne, Heidelberg, VIC 3084, Australia
[f] Protein Crystallography Program, Oklahoma Medical Research Foundation, Oklahoma City, OK 73104, United States

ARTICLE INFO

Article history:
Received 25 November 2010
Received in revised form 1 March 2011
Accepted 8 March 2011
Available online 3 April 2011

Keywords:
Immunoglobulin light chain
Immunotherapy
Antibody
Epitope
Molecular modelling

ABSTRACT

The murine mAb, K-1-21, recognizes a conformational epitope expressed on free Ig kappa light chains (FκLCs) and also on cell membrane-associated FκLCs found on kappa myeloma cells. This has led to the development of a chimeric version of K-1-21, MDX-1097, which is being assessed in a Phase II clinical trial for the treatment of multiple myeloma. The epitope recognized by K-1-21 is of particular interest, especially in the context that it is not expressed on heavy chain-associated light chains such as in an intact Ig molecule. Using epitope excision techniques we have localized the K-1-21 epitope to a region spanning residues 104–110 of FκLC. This short strand of residues links the variable and constant domains, and is a flexible region that adopts different conformations in FκLC and heavy chain-associated light chain. We tested this region using site-directed mutations and found that the reactivity of K-1-21 for FκLC was markedly reduced. Finally, we applied *in silico* molecular docking to generate a model that satisfied the experimental data. Given the clinical potential of the Ag, this study may aid the development of next generation compounds that target the membrane form of FκLC expressed on the surface of myeloma plasma cells.

1. Introduction

Therapeutic mAbs represent the largest class of biological agents with widespread use in oncology and autoimmunity. Each Ab is unique, and can function through many mechanisms such as inducing apoptosis, recruitment of effector cells and complement, and blocking interactions between receptors and ligands that are vital for activation of a target cell (Piggee, 2008). Understanding the modes by which Abs interact with their cognate Ags is invaluable for future developments in Ab based therapeutics. Unfortunately, many Ab–Ag complexes fail to crystallise and their structures cannot be determined by high resolution X-ray diffraction. Complicating the matter further, most protein-binding Abs recognize targets through conformational epitopes, and conventional mapping techniques are limited (Caoili, 2010; Chen et al., 2009; Kiselar and Downard, 1999; Saul and Alzari, 1996). One such Ab is the murine mAb, K-1-21, which recognizes a conformational epitope on human free Ig kappa light chains (FκLC), but does not recognise kappa light chains (κLC) that are in association with Ig heavy chain (HC) such as in an intact Ig molecule (Boux et al., 1983; Raison and Boux, 1985).

In humans, there are two isotypic variants of light chain (LC), kappa and lambda with 65% of B cells expressing the former (Barandun et al., 1976; Bradwell et al., 2008). LCs are composed of two beta-sheet rich Ig domains, the variable (V) and constant (C) domains that are connected by a short strand referred to as the 'switch' region (Schiffer et al., 1973). In an Ab molecule, the V domain of LC, in conjunction with the V domain of the associated heavy chain (HC), forms the Ag binding site. Diversity in the LC V domain is achieved by shuffling and recombination of individual germline gene segments, the variable and joining genes, during B cell development. The recombined V domain is then fused to the

* Corresponding author at: School of Medical and Molecular Biosciences, University of Technology Sydney, PO Box 123, Ultimo, NSW 2007, Australia.
Tel.: +61 2 9514 1789; fax: +61 2 9514 8206.
E-mail address: andrew.hutchinson@uts.edu.au (A.T. Hutchinson).
[1] Equal contribution to this work.

0161-5890/$ – see front matter.
doi:10.1016/j.molimm.2011.03.003

C domain which does not undergo recombination events (Abbas et al., 2007).

During the process of Ab synthesis, LCs are produced in excess of HCs which causes the secretion of FLCs by plasma cells (Bradwell et al., 2008; Hopper and Papagiannes, 1986). FLCs exist in three forms: as covalent and non-covalent homodimers, formed via interactions of adjacent V and C domains, and as free monomers (Bradwell et al., 2008). High levels of FLC in serum can be indicative of an underlying plasma cell malignancy such as multiple myeloma (Bradwell et al., 2008; Mead et al., 2004). Furthermore, analysis with mAb K-1-21 has shown that FκLCs are bound to sphingomyelin on the cell membrane of myeloma plasma cells (Goodnow and Raison, 1985; Hutchinson et al., 2010; Walker et al., 1985). This has led to the development of a chimeric form of K-1-21, termed MDX-1097, that is currently undergoing assessment in a Phase II clinical trial for the treatment of multiple myeloma (Australian New Zealand Clinical Trials Registry Number: 12610000700033).

Although early studies on the characterization of K-1-21 suggested that the Ab recognizes a conformational epitope located in the C domain of FκLC (Raison and Boux, 1985), it remains to be elucidated how the mAb interacts with FκLC but fails to recognize HC-associated forms of κLC as found in an Ig molecule or an Fab fragment (Boux et al., 1983) (see Supplementary Fig. 1). In this study, we utilized a range of techniques to identify regions on FκLC that may comprise the epitope recognized by K-1-21. Using the experimental data, we then applied *in silico* molecular docking to arrive at a suitable model for the Ab–Ag complex formed between K-1-21 and FκLC.

2. Materials and methods

2.1. General reagents

K-1-21 was produced on a fee for service basis by the Australian Commonwealth Scientific and Industrial Research Organization. FκLC were purified from the urine of MM patients by ammonium sulfate precipitation as described previously (Raison and Boux, 1985). Monomers and dimers of FκLC in these preparations were separated by size exclusion chromatography.

2.2. K-1-21 affinity purification of in situ derived FκLC peptides

FκLC peptides that had undergone proteolysis whilst being stored in urine were affinity purified by passage over a K-1-21 CNBr-activated Sepharose column (GE Biosciences). Purified peptides were subjected to two-dimensional electrophoresis. Briefly, samples were separated on a 3–10 pI immobilized gradient strip (BioRad), then size separated by SDS–PAGE in a 4–12% Criterion XT gel (BioRad). Gels were stained with Flamingo fluorescent stain (BioRad) and imaged on a Pharos FX Plus Molecular Imager (BioRad). Spots containing relevant peptides were excised from the gel and trypsinised for nanoLC/MS–MS analysis which was performed by the Australian Proteome Analysis Facility (APAF), at Macquarie University, NSW.

2.3. Epitope excision

Epitope excision was performed essentially following the protocol described by Parker and Tomer (2000). Briefly, K-1-21 was immobilized on CNBr-Sepharose then incubated with 50 μg FκLC for 2.5 h at room temperature. Unbound Ag was washed away and trypsin was added at a 1:20 w/w enzyme–substrate ratio. The digestion was carried out at 37 °C for 24 h with slow rotation. Trypsin and unbound peptides were removed by washing the columns with PBS prior to performing the MS analysis. In addition, FκLC was incubated with trypsin in solution for use as a positive control for tryptic digestion.

MALDI-MS was performed on a Voyager-DE STR (PerSeptive Biosystems) instrument equipped with a nitrogen laser (337 nm). The accelerating voltage was set at 20 kV and spectra were acquired by averaging data of 100 laser shots. Sepharose beads (15 μL) were loaded on a C18 ZipTip (Millipore), washed three times with 0.1% TFA and bound peptides were eluted with 2 μL of matrix solution. Only peptides in the detection range of 600–5000 Da were analysed. Peptides present in the mass spectra were identified by a Mascot search for tryptic peptides with the same mass against a human or mouse protein database, allowing ±3 Da error and up to 3 missed cleavage sites.

2.4. Site-directed mutagenesis and expression of FκLC constructs

The κLC gene was amplified from JJN-3 cell line cDNA with forward and reverse primers comprising the sequence 5′-CACCATGGAAACCCCAGCG-3′ and 5′-CTAGCACTCTCCCCTGTTG-3′ respectively. Using this as a template, internal mutagenic primers were designed (see Supplementary Table 2), and mutated constructs were amplified using κLC specific primers with the various mutagenic primers. PCR products were cloned into the entry vector pENTR/D-TOPO then subcloned into the pT-Rex/DEST30 vector according to the manufacturer's recommendations (Invitrogen). Truncated κLC constructs were synthesized by GENEART, Germany. Purified expression plasmids were transfected into HEK-293 cells using the Freestyle Max expression system (Invitrogen). At Day 3, supernatants were collected and analysed by surface plasmon resonance.

2.5. Testing the reactivity of K-1-21 to mutated FκLC constructs

The binding reactivity of K-1-21 to FκLC constructs was assessed by surface plasmon resonance on a Biacore 2000 (GE Biosciences). K-1-21, polyclonal anti-κLC (Sigma) and polyclonal anti-λLC (isotype control; Sigma) were covalently coupled to the surface of a CM5 sensor chip (GE Biosciences). Cell supernatants from κLC transfected HEK-293 cells were injected for 10 min at a flow rate of 20 μL/min, followed by a stabilization step for 10 min. The surface was regenerated by injecting 10 mM glycine, pH 1.8 for 30 s at a flow rate of 100 μL/min. K-1-21 and anti-κLC arbitrary response units for each FκLC construct were standardized with reference to a FκLC standard curve, then expressed as a percentage of the FκLC control transfectant.

2.6. Derivation of molecular models and docking studies

A homology model of the K-1-21 Fv (VL and VH domains) was constructed using the homology module of the Insight II program suite, version 98 (Accelrys, San Diego, CA, USA). Templates for the models were selected from the Protein Data Base (PDB) on the basis of sharing high amino acid similarities and CDRs of the same lengths and canonical structures to the sequences being predicted (Ramsland et al., 1997, 1999, 2001). Templates used to generate the K-1-21 Fv were from PDB codes: 12E8 for VL and 2RCS for VH (coordinates for the CDR3 of the HC were from 1BFV). The initial template-based K-1-21 Fv model was generated using the Modeller algorithm (Sali and Blundell, 1993), which was subjected to conjugate-gradient energy minimization until convergence to an energy gradient of 0.001 kcal/mol using the Crystallography and NMR System (Brunger et al., 1998). Harmonic restraints of 10.0 kcal/(mol Å^2) were imposed on all main chain heavy atoms during the energy minimization simulations.

A homology model of a covalent κLC dimer was generated using procedures similar to those outlined above, however, the Discovery Studio package, version 2.5 (Accelyrs, USA) was used to prepare and optimize the model. Briefly, the V and C domains from the Del κLC (PDB: 1B6D) were superimposed onto the 1.9 Å resolution structure of the Sea covalent λLC dimer, PDB: 1JVK (Bourne et al., 2002; Terzyan et al., 2003). An interchain disulfide linkage was introduced linking the two κLC monomers and the model was optimized by the Modeller algorithm and energy minimization within Discovery Studio.

Rigid body molecular docking was performed with the ClusPro 2.0 algorithm (http://cluspro.bu.edu/) using K-1-21 as the receptor and chain B of the FκLC non-covalent dimer, PDB: 1B6D, as the ligand (Comeau et al., 2007). Attraction regions were set on the κLC comprising the residues 105–109 in the switch region, and the algorithm was run in Ab mode with the non-CDR regions masked in K-1-21. An appropriate model was chosen based on having a low energy 'best fit' score and whether κLC switch residues made contact with K-1-21 CDRs (therefore satisfying the experimental data). The derived model was then optimized by the RosettaDock algorithm (http://rosettadock.graylab.jhu.edu/) which takes into account sidechain flexibility (Lyskov and Gray, 2008; Schueler-Furman et al., 2005).

2.7. Kinetic analysis and determination of affinity constants

For kinetic studies, we utilised an anti-Fc mAb capture method to determine affinity constants. The advantage of this approach is that it prevents the mAb surface from degradation between cycles due to the low pH in the regeneration buffer. As such, new mAb is captured onto the chip before each run. In brief, goat anti-mouse Ab (Sigma) was immobilized to the surface of a CM5 chip (GE Biosciences). K-1-21 at 10 μg/mL was injected for 1.5 min at 30 μL/min and the surface was stabilized for 10 min. This was followed by triplicate injections of FκLC monomers, covalent and non-covalent dimer at concentrations ranging from 500 nM to 3.9 nM for 5 min. Dissociation for 15 min was followed by regeneration with 10 mM glycine pH 1.8 for 45 s at 100 μL/min flow rate. The data was fitted to a 1:1 Langmuir binding model using the BiaEvaluation 3.1 software (GE Biosciences) and the calculated kinetic values were regarded as acceptable at $Chi^2 < 2$ and residuals in the range of −2 to +2.

3. Results

3.1. The K-1-21 epitope comprises part of the C domain of FκLC

We had previously identified a kappa Bence Jones protein (FκLC) that had undergone proteolytic digestion whilst being stored in urine (presumably by proteases present in the sample). Analysis of this material using a K-1-21 affinity column yielded a number of κLC fragments that were reactive with K-1-21. In order to identify these peptides, K-1-21 affinity purified κLC fragments were subject to 2D electrophoresis. Two groups of peptides were present in the K-1-21 purified material; a monomeric FκLC population migrating at approximately 25 kDa and peptides with apparent MW between 10 and 15 kDa (Fig. 1A). Of these lower MW peptides, four spots were selected for further analysis and following gel extraction and tryptic digestion, were analysed by LC/MS.

Alignment of the tryptic peptides from the four samples revealed that the smallest peptide within which the epitope was retained yielded a sequence that commenced at R108 and terminated at K183 (Fig. 1B and Supplementary Table 1). This ruled out the C-terminal region from K183 onwards as being involved in the epitope. However, the N-terminal residue of this peptide could not be unequivocally assigned because the amino acid immediately preceding R108 is K107. Furthermore, in all κLCs there is a primary amine at 103 (either lysine for JK1, JK2, JK3 and JK4 gene segments, or an arginine for the JK5 gene segment). Since the peptide samples were trypsinized before identification by LC/MS, cleavage at residues 103 and 107 is unlikely to have yielded detectable peptides in the LC/MS analysis. In support of this, we note that a FκLC peptide spanning residues 108–183 would have an estimated mass of 8 kDa which is smaller than the actual mass of the peptide as shown by SDS–PAGE (between 10 and 15 kDa; Fig. 1B). As such, it is likely that N-terminal residues preceding R108 were present but not identified as a result of tryptic digest.

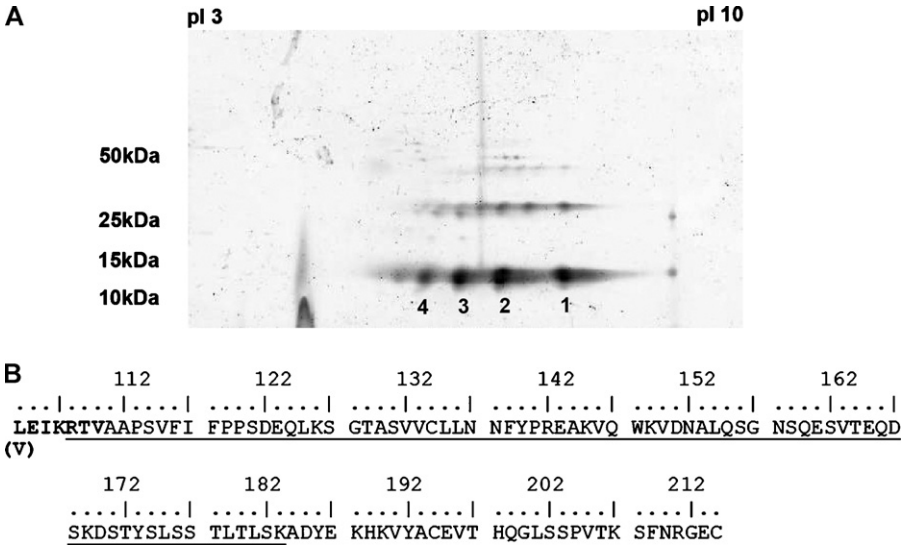

Fig. 1. Identification of K-1-21 affinity purified FκLC peptides. FκLC that had undergone some proteolytic digestion *in situ*, was affinity purified by Sepharose-conjugated K-1-21. (A) The eluted fraction was subject to 2D electrophoresis then spots corresponding to fragments of κLC (approximately 10–15 kDa) were cut out for analysis by nanoLC/MS–MS. (B) κLC sequence showing the C domain and the switch region (residues 104–214). Underlined residues represent the smallest K-1-21 specific *in situ* derived peptide as identified by nanoLC/MS–MS. Residues in bold correspond to switch region fragments identified by epitope excision (see Supplimentary Fig. 2). Note residue 104 can be either a leucine or valine due to variability in κLC joining gene segments.

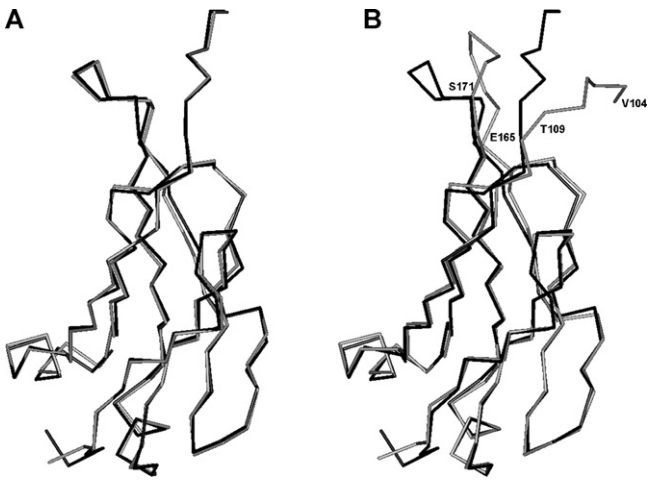

Fig. 2. Comparison of peptide backbones in FκLC and HC-associated κLC C domains. (A) C domain overlay of chain A 1B6D FκLC (grey) with κLC of 2FGW Fab (black). (B) C domain overlay of chain B 1B6D FκLC (grey) with κLC of 2FGW Fab (black).

3.2. The switch region in FκLC is protected by K-1-21 during trypsin digest

Epitope excision was undertaken in order to further define the location of the epitope. The nature of this experiment relies on the protection of the antigenic determinant from enzymatic proteolysis when an Ag–Ab complex is formed. The success of such epitope protection assays is determined by the resistance of the Ab to digestion (Parker and Tomer, 2000).

FκLC bound to K-1-21 immobilised on Sepharose were digested with trypsin and, after washing, peptides bound to the Ab on the beads were identified by MALDI-MS and Mascot database search. The smallest peptide (656.09 Da; LEIKR) was identified as part of the switch region (residues 104–108, the junction between V and C domains). This sequence is identical in both human and murine κLC, thus it was possible that this peptide originated from either the Ab or the Ag, or both (Fig. 1B and Supplementary Fig. 2). However, exhaustive washing of the Sepharose-immobilized complex subsequent to proteolysis and prior to MALDI-MS, should eliminate any peptides originating from the Sepharose-bound K-1-21. Furthermore, this peptide was not present in the mass spectrum of FκLC digested in the absence of K-1-21 (see Supplementary Fig. 2), suggesting that the cleavage site between K107 and R108 was protected when FκLC is bound to K-1-21. A slightly larger peptide (862.14 Da) was also observed to be bound to the immobilized Ab and was identified as an overlapping sequence, LEIKRTV (residues 104–110). This sequence is unique for human κLC and probably resulted from non-specific cleavage after V110 (Fig. 1B and Supplementary Fig. 2). Again, this result suggested that epitope protection had taken place. Numerous other peptides were present at much lower peak intensities and were assigned as murine (K-1-21) HC and LC V region sequences (see Supplementary Fig. 2).

3.3. Comparisons of κLC structures reveal a conformational change at the switch region in FκLCs

The unique specificity of K-1-21 to FκLC rather than HC-associated κLC suggests there are conformational differences between the two forms of the molecule. We compared the structures of a FκLC non-covalent dimer, PDB: 1B6D, with a HC-associated κLC derived from the Fab, PDB: 2FGW. Interestingly, chain A of 1B6D dimer overlaid remarkably well with 2FGW κLC indicating they are very similar in conformation (Fig. 2A). In contrast, the backbone of chain B in 1B6D dimer markedly deviated from the Fab κLC in two places: at the switch region comprising the residues 104–109 and at a loop, spatially adjacent to this region, consisting of residues 165–171 (Fig. 2B). Fig. 3 highlights these regions in more detail. As shown, residues 104–109 and 165–171 of chain B of 1B6D dimer differ greatly in conformation in comparison to the corresponding regions found in 2FGW κLC and chain A of 1B6D. Moreover, when looking at the position of the V and C domains in chain B, it becomes apparent that much of this conformational change can be attributed to a more acute angle formed between the two domains. As regions 104–109 and 165–171 in chain B are the only sites on FκLC that are conformationally different to HC-associated κLC, it reinforces the possibility that this region comprises the epitope bound by K-1-21.

3.4. Mutation and truncation of FκLC residues confirms the switch region as an essential component of the epitope

Epitope excision and structural comparisons of κLC highlighted the switch region and the adjacent loop as a putative epitope bound by K-1-21. In order to further define the epitope, we used site-directed mutagenesis and polypeptide truncation to identify critical residues involved in the binding of K-1-21 to FκLC. The κLC from the JJN3 myeloma cell line was cloned and the product expressed transiently in HEK-293 cells. Importantly, the expressed product retained the epitope bound by K-1-21 and also reacted with a polyclonal anti-κLC Ab as determined by Biacore biosensor analysis.

The κLC constructs outlined in Table 1 were expressed and tested for reactivity with K-1-21 and polyclonal anti-κLC. Arbitrary response units of the recombinant proteins to K-1-21 and polyclonal anti-κLC on the sensor chip were standardized with reference to a FκLC standard curve then expressed as a percentage of the control full length recombinant κLC (Table 1). The C domain construct showed reactivity to K-1-21 and polyclonal anti-κLC of 43% and 44%, respectively. These values were consistent with this fragment being approximately half the mass of the full length FκLC, and thus resulting in values that are approximately half the full length FκLC control. This interpretation was confirmed by the fact that the ratio of the reactivity of K-1-21 and the polyclonal Ab to this fragment (0.98) was similar to that of the full length FκLC control. This confirmed that the K-1-21 epitope is retained in the peptide commencing at residue V104 and extending to the penultimate residue 214. To further define the K-1-21 epitope we generated and expressed another truncated κLC construct beginning at residue K107 for comparison with the construct described above that contained the entire switch region (Table 1). Interestingly, removal of just the first three residues (104–106) almost completely abolished the reactivity of K-1-21 to the truncated κLC (K-1-21 to polyclonal anti-κLC binding reactivity ratio of 0.12; Table 1) confirming the critical role of these residues in defining the K-1-21 epitope.

Mutation of either E105 or T109 to alanine in the full length κLC construct resulted in significant reduction in the ability of K-1-21 to recognize the polypeptide. The reactivity of K-1-21 was 36% and 28% for the E105A and T109A mutations respectively when compared to the non-mutated control. These mutations had significantly less effect on reactivity with polyclonal anti-κLC (78% for E105A and 67% for T109A). Although these lower values could be attributed to low FκLC expression levels by the transfected mutants, the large discrepancy in reactivity values between K-1-21 and anti-FκLC suggest that part of the K-1-21 epitope had been affected. This was highlighted in the FκLC reactivity ratio of K-1-21 to the polyclonal anti-κLC was reduced to 0.46 for E105A and 0.42 for T109A indicating that the effect of the mutations was largely restricted to the epitope recognized by K-1-21.

It was noted that κLCs derived from the JK3 segment contain an aspartic acid at 105 (found in approximately 5% of κLC sequences;

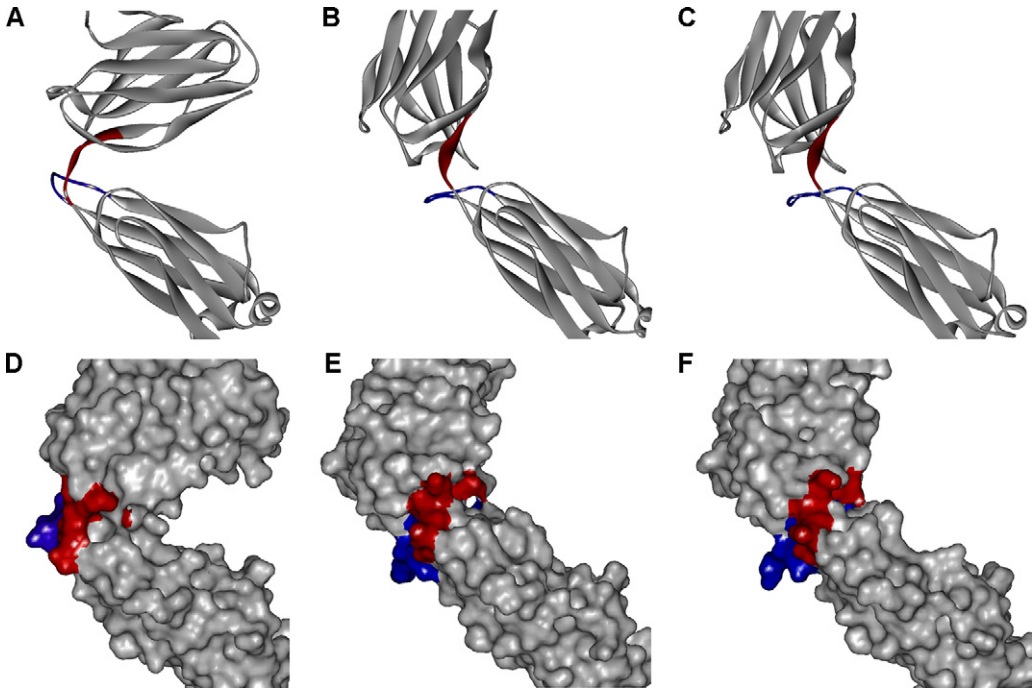

Fig. 3. Surface and ribbon diagrams of the proposed epitope region on κLC. (A–C) Ribbon diagrams, (D–F) surface diagrams. Chain B 1B6D dimer: A and D. Chain A 1B6D dimer: B and E. LC 2FGW Fab: C and F. Red highlighted residues constitute the switch region (residues 104–109) and blue highlighted residues are the adjacent loop (residues 165–171). (For interpretation of the references to color in this figure legend, the reader is referred to the web version of the article.)

Kabat et al., 1992) rather than a glutamic acid. As this residue was shown to be a key component of the epitope for K-1-21, it may have an impact on the clinical utility of MDX-1097 (the human chimeric equivalent of K-1-21) for a subset of myeloma patients. Therefore it was necessary to confirm that K-1-21 can still interact with κLCs that have an aspartic acid at 105. Interestingly, mutation of E105 to aspartic acid resulted in enhanced binding of K-1-21 to FκLC as indicated by a high reactivity ratio of 1.70 for K-1-21 versus the polyclonal anti-κLC (Table 1). Thus we can conclude that MDX-1097 will retain reactivity to myeloma cells expressing κLCs with D105.

We also tested the role of the region around residues 165–171 by shuffling the native sequence DSKD (residues 167–170) to KDDS. For this construct the ratio of K-1-21 binding reactivity to anti-κLC reactivity was 0.79 which indicated that the epitope was only partially affected (Table 1). To further define this region, we mutated Q166 to a proline in order to locally disrupt the conformation of the peptide chain. Interestingly, this mutation had no effect on the ability of K-1-21 to bind FκLC (Table 1). Although this data suggests that the loop comprising the residues 165–171 does not play a definitive role in the K-1-21 epitope, it is still possible this region may be part of the conformational epitope, but plays little role in the specificity of K-1-21.

3.5. Model derivation and analysis

To test the proposed role of the switch region in the K-1-21 epitope, we used *in silico* molecular docking to probe this region, and to derive an appropriate model for the K-1-21–FκLC complex. Initially we derived a structure of the K-1-21 Fv based on homology modelling. The K-1-21 Fv model was then docked onto the non-covalent FκLC dimer 1B6D with the ClusPro 2.0 algorithm (Comeau et al., 2007).

We found that K-1-21 could be docked onto the proposed epitope in chain B of 1B6D. In this model, T109 is found buried deep in a hydrophobic binding pocket of K-1-21 formed by multiple tyrosine residues. In addition, a potential hydrogen bond (H-bond) occurs between T109 and V100 in K-1-21 HC. K107 side chain atoms interact via van der Waals forces with N32 and Y91 of K-1-21 LC, and the aromatic ring of Y104 in K-1-21 HC is found in close association with backbone atoms of K107. Main chain atoms between K107 and R108 form H-bonds with Y91 of K-1-21 LC. R108, in the proposed epitope, forms another H-bond with the side chain Y33 in K-1-21 HC, which is stabilized by van der Waals contacts between the side chains of Y101 in K-1-21 HC. Additionally, Y101 of K-1-21 HC also forms an H-bond with backbone atoms of K169 (Fig. 4A and B).

Table 1
Reactivity of recombinant FκLC constructs to K-1-21 and polyclonal anti-κLC.

Construct	Description	Reactivity (% of κLC control)		Ratio[a]
		K-1-21	Anti-κLC	
κLC	Full length κLC control	100	100	1
VEIKRTV + C domain	Residues 104–214	43	44	0.98
KRTV + C domain	Residues 107–214	5	43	0.12
E105A	E105 mutated to A	36	78	0.46
T109A	T109 mutated to A	28	67	0.42
E105D	E105 mutated to D	135	79	1.70
KDDS	DSKD (167–170) shuffled to KDDS	67	85	0.79
Q166P	Q166 mutated to P	91	92	0.99

[a] Defined as the ratio of K-1-21 and anti-κLC reactivity to the various κLC constructs.

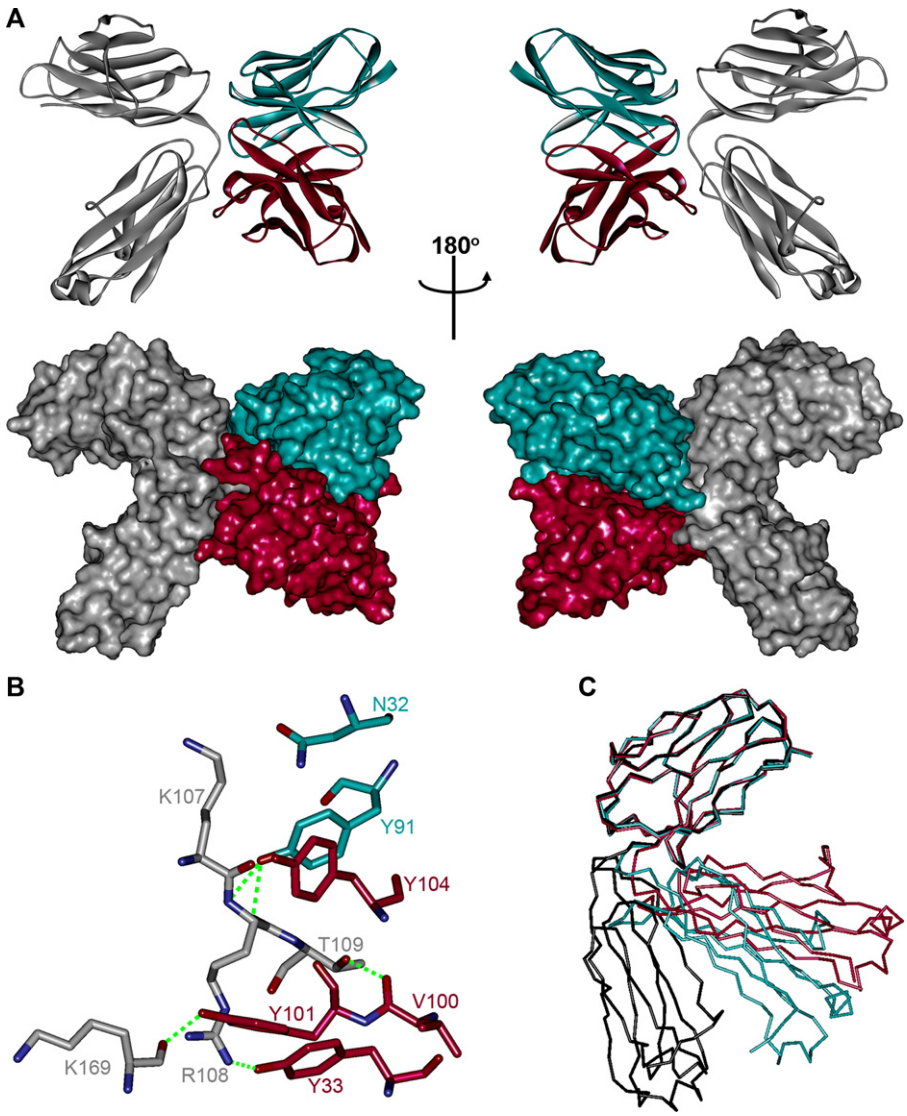

Fig. 4. K-1-21 Fv bound to FκLC model. (A) Surface and ribbon diagrams of the model. Magenta and cyan structures denote the K-1-21 HC and LC respectively. Grey denotes chain B of 1B6D non-covalent dimer. (B) Key interactions taking place between K-1-21 Fv and the switch region of 1B6D non-covalent dimer. Atoms are colored by type (1B6D carbon, grey; K-1-21 HC carbon, magenta; K-1-21 LC carbon, cyan; nitrogen, blue; oxygen, red). H-bonds are shown as green dashed lines. (C) Carbon-alpha trace V domain overlays of chain B κLC 1B6D (magenta), chain B covalent dimer model (cyan) and κLC chain of 2FGW Fab (black). (For interpretation of the references to color in this figure legend, the reader is referred to the web version of the article.)

In contrast to this model, K-1-21 failed to dock onto the same region in chain A. As chain A shares a similar conformation to HC-associated κLC (Figs. 2 and 3), we also tested whether κLC Fabs could be docked into the K-1-21 Fv. Similar to chain A of 1B6D, none of these Fabs were able to dock via their switch regions to K-1-21. This further highlights the unique conformation of the proposed epitope in chain B of 1B6D FκLC.

In addition, we attempted docking K-1-21 to a model of a covalent FκLC dimer with both LCs in an extended conformation compared to chain B of 1B6D. Again, the algorithm failed to dock K-1-21 Fv to either of the κLC switch regions. This was an unexpected result, since K-1-21 has been shown to bind to covalently associated FκLC dimers (Raison and Boux, 1985). In this model, the switch region of chain A is similar to HC-associated κLC (and chain A of 1B6D dimer). However, chain B of the covalent dimer is different to chain B from the non-covalent dimer 1B6D. This is partly due to a more extended conformation of the V and C domains in the covalent dimer (Fig. 4C). Thus K-1-21 binding to a covalent κLC may require a conformational change in the switch region inducing a more acute angle between the V and C domains. Access to the K-1-21 epitope on covalent κLC is still predicted to be feasible since, in the model, one LC monomer displays a conformation closer to the acutely bent κLC of the non-covalent dimer than to the extended κLC associated with the HC in a Fab (Fig. 4C).

Subsequently, we have measured the affinity of K-1-21 binding to monomers, covalent dimers and non-covalent dimers of FκLC by plasmon resonance. We found that K-1-21 has higher affinity for non-covalent dimers than monomers and covalent dimers (Table 2). This indicates that the conformation of the K-1-21 epitope in non-covalent dimers is more accessible for binding to K-1-21. In addition, these data support the concept that induced fit plays a dominant role in K-1-21 binding to covalent κLC dimers. This

Table 2
Kinetic constants for the interaction between K-1-21 and FκLCs.

	k_a (M^{-1} s^{-1})	k_d (s^{-1})	K_A (M^{-1})	K_D (M)
Non-covalent dimers	15.3×10^4	1.05×10^{-3}	14.5×10^7	6.9×10^{-9}
Covalent dimers	9.98×10^4	1.96×10^{-3}	5.09×10^7	19.6×10^{-9}
Monomers	3.64×10^4	0.74×10^{-3}	4.87×10^7	20.6×10^{-9}

is highlighted by the finding that the rigid-body docking program was unable to generate complexes of the K-1-21 Fv with the switch regions of the covalent κLC dimer model. It is therefore possible that a small conformational change in the switch region may be necessary to allow the binding of covalent dimers to K-1-21.

4. Discussion

Previous studies have shown that K-1-21 recognizes a conformational epitope located in the C domain of FκLC. Interestingly, it does not recognize HC-associated κLC (in the form of an Ab molecule or Fab), which suggests there are conformational differences between the two forms of the molecule (Raison and Boux, 1985). In this work, we initially used epitope excision with tryptic digestion to further define the region recognized by K-1-21. This yielded two overlapping peptides that were protected from tryptic digestion. These peptides encompassed residues L104 to V110 that make up the switch region connecting the V and C domain of κLC.

By analysing structures of HC-associated κLC and FκLC, we noted that the switch region and a spatially adjacent loop (residues 165–171) were conformationally different in the two forms of the molecule. Mutagenesis was then utilized to further examine the potential role of these regions in the epitope. It was found that alanine mutations at switch residues E105 and T109, reduced the reactivity of K-1-21 to FκLC by more than 50% (based on the ratio of K-1-21 reactivity to the polyclonal anti-κLC reactivity). Furthermore, a partial switch deleted mutant (C domain commencing at K107) showed minimal binding to K-1-21, thus confirming that the switch region contains residues critical to the integrity of the epitope. To analyse the role of the adjacent loop, a shuffle mutant was expressed (residues 167–170 shuffled from DSKD to KDDS) that showed a small but definitive reduction in the ability to bind to K-1-21. However, mutating Q166 to proline, in order to disrupt the peptide chain, showed no effect on K-1-21 reactivity. Together these results suggest this region is not critical to the epitope, but may provide a supporting role in the K-1-21 interaction with FκLC.

In the absence of an X-ray crystal structure, we derived a model of K-1-21 Fv based on previously solved structures of homologous mAbs. We next utilized the rigid-body molecular docking algorithm ClusPro 2.0 to determine whether the switch region could be accommodated in the binding site of K-1-21 (Comeau et al., 2007). A best-fit model was selected based on a combination of having low energy (highly ranked docking poses) and whether it was supported by the experimental data. The semi-rigid RosettaDock algorithm, which allows side chain flexibility (Schueler-Furman et al., 2005), was then used to further refine the model. The model we derived was consistent with our experimental data. T109, one of the key residues in the mutagenesis study, was found buried deep in the tyrosine-rich binding pocket of K-1-21, with an H-bond formed between the side chain of T109 and the backbone of V100 in the K-1-21 HC. Other important contact residues in the epitope were K107 and R108. Notably, these residues were protected by tryptic digest in the epitope excision experiment, which suggests they are located in the binding site of K-1-21. It is interesting to note that E105, which was thought to be a key component of the epitope based on the mutagenesis study, makes no contact with K-1-21 in the model. However, this residue is close to 107–109 (KRT residues) and may provide part of the scaffold for appropriate presentation of the contact residues to K-1-21. This is supported by the finding that a truncated form of κLC, which begins at K107, and therefore does not have E105, fails to bind to K-1-21 indicating the loss of the epitope. Interestingly, K169 was found H-bonded with Y101 in K-1-21 HC. Seeing this interaction was mediated by main chain atoms rather than the side chain of K169, this suggests that a number of different residues may be substituted into this region without compromising the interaction with K-1-21. In support of this is the observation that various mutations in the loop comprising residues 166–170 showed little effect on K-1-21 binding. As such, it cannot be ruled out that this region does not play a definitive role in the epitope, however the interaction may be via an induced fit mechanism allowing for a range of different amino acids to be substituted into the peptide loop.

In addition, we also tried docking K-1-21 Fv with HC-associated κLCs, to which the mAb does not bind (Boux et al., 1983) (see Supplementary Fig. 1), and did not find any model in which K-1-21 bound to the κLC via similar mechanisms. This further highlights the conformational nature of the epitope. Molecular docking also failed to find an appropriate model for K-1-21 bound to covalent FκLC dimer. Experimental evidence shows that covalent FκLCs can bind to K-1-21, albeit with lower affinity than non-covalent dimers. Combined with the docking results we suggest that conformational changes are required for covalent FκLC dimers to interact with K-1-21. Perhaps the κLC require a bent or acute conformation (with respect to the V and C domains) before they can bind K-1-21, which explains the unique specificity of this Ab for human FκLC.

In addition to soluble FκLC, K-1-21 is highly specific for a cell surface determinant called KMA (kappa myeloma Ag) that consists of a complex of aggregated FκLC bound to sphingomyelin (Hutchinson et al., 2010). KMA is expressed on a range of B cell malignancies, and the chimeric version of K-1-21, MDX-1097, is currently being assessed in a Phase II clinical trial for multiple myeloma (Australian New Zealand Clinical Trials Registry Number: 12610000700033). Given KMA's therapeutic potential as a tumour-specific Ag, our findings are of interest in that the identified epitope region could be used for the rationale design of 'next generation' anti-KMA therapeutics. Developing new therapeutic agents targeting KMA is not straightforward given that κLCs are also part of intact Ig molecules that are a major component of the B cell receptor that is expressed on most B cell subsets. Thus our determination of the K-1-21 epitope, which is unique to FκLC rather than HC-associated κLC, may be of great benefit in future screening or immunisation strategies for the development of anti-KMA compounds.

In summary, we have utilized a number of experimental techniques to locate the epitope on FκLC that is recognised by K-1-21. Using this information, we then applied *in silico* molecular docking to arrive at a suitable model for the K-1-21 mAb–FκLC complex. In the absence of an empirically solved molecular structure, this approach may be suitable for the derivation of models for many other Ab–Ag complexes.

Conflict of interest

A.T.H., D.R.J., C.V.J., and R.L.R. are previous employees of Immune System Therapeutics Ltd. K.B. and A.B.E. have served in an advisory role to Immune System Therapeutics Ltd. A.T.H., D.R.J., C.V.J., K.B., A.B.E., and R.L.R. own stock in Immune System Therapeutics Ltd.

Acknowledgements

This work was funded by Immune System Therapeutics Ltd., Australia. P.A. Ramsland is a recipient of an R. Douglas Wright Career Development Award (ID365209) from the National Health and Medical Research Council of Australia (NHMRC). The authors gratefully acknowledge the contribution to this work of the Victorian Operational Infrastructure Support Program received by the Burnet Institute.

Appendix A. Supplementary data

Supplementary data associated with this article can be found, in the online version, at doi:10.1016/j.molimm.2011.03.003.

References

Abbas, A.K., Lichtman, A.H., Pillai, S., 2007. Cellular and Molecular Immunology. Elsevier, Amsterdam, Netherlands.

Barandun, S., Morell, A., Skvaril, F., Oberdorfer, A., 1976. Deficiency of kappa-or lambda-type immunoglobulins. Blood 47, 79.

Bourne, P., Ramsland, P., Shan, L., Fan, Z., DeWitt, C., Shultz, B., Terzyan, S., Moomaw, C., Slaughter, C., Guddat, L., 2002. Three-dimensional structure of an immunoglobulin light-chain dimer with amyloidogenic properties. Acta Crystallogr. D: Biol. Crystallogr. 58, 815–823.

Boux, H.A., Raison, R.L., Walker, K.Z., Hayden, G.E., Basten, A., 1983. A tumor-associated antigen specific for human kappa myeloma cells. J. Exp. Med. 158, 1769–1774.

Bradwell, A.R., Mead, G.P., Carr-Smith, H.D., 2008. Serum Free Light Chain Analysis. The Binding Site, Birmingham, UK.

Brunger, A., Adams, P., Clore, G., DeLano, W., Gros, P., Grosse-Kunstleve, R., Jiang, J., Kuszewski, J., Nilges, M., Pannu, N., 1998. Crystallography & NMR system: a new software suite for macromolecular structure determination. Acta Crystallogr. D: Biol. Crystallogr. 54, 905–921.

Caoili, S., 2010. Benchmarking B-cell epitope prediction for the design of peptide-based vaccines: problems and prospects. J. Biomed. Biotechnol., 910524.

Chen, S., Van Regenmortel, M., Pellequer, J., 2009. Structure–activity relationships in peptide–antibody complexes: implications for epitope prediction and development of synthetic peptide vaccines. Curr. Med. Chem. 16, 953–964.

Comeau, S.R., Kozakov, D., Brenke, R., Shen, Y., Beglov, D., Vajda, S., 2007. ClusPro: performance in CAPRI rounds 6–11 and the new server. Proteins 69, 781–785.

Goodnow, C.C., Raison, R.L., 1985. Structural analysis of the myeloma-associated membrane antigen KMA. J. Immunol. 135, 1276–1280.

Hopper, J.E., Papagiannes, E., 1986. Evidence by radioimmunoassay that mitogen-activated human blood mononuclear cells secrete significant amounts of light chain Ig unassociated with heavy chain. Cell. Immunol. 101, 122–131.

Hutchinson, A.T., Ramsland, P.A., Jones, D.R., Agostino, M., Lund, M.L., Jennings, C.V., Bockhorni, V., Yuriev, E., Edmundson, A.B., Raison, R.L., 2010. Free immunoglobulin light chains interact with sphingomyelin and are found on the surface of myeloma plasma cells in an aggregated form. J. Immunol. 185, 4179–4188.

Kabat, E.A., Te Wu, T., Perry, H.M., Gottesman, K.S., Foeller, C., 1992. Sequences of Proteins of Immunological Interest. DIANE Publishing.

Kiselar, J., Downard, K., 1999. Direct identification of protein epitopes by mass spectrometry without immobilization of antibody and isolation of antibody–peptide complexes. Anal. Chem. 71, 1792–1801.

Lyskov, S., Gray, J.J., 2008. The RosettaDock server for local protein–protein docking. Nucleic Acids Res. 36, W233–W238.

Mead, G.P., Carr-Smith, H.D., Drayson, M.T., Morgan, G.J., Child, J.A., Bradwell, A.R., 2004. Serum free light chains for monitoring multiple myeloma. Br. J. Haematol. 126, 348–354.

Parker, C., Tomer, K., 2000. Epitope mapping by a combination of epitope excision and MALDI-MS. Methods Mol. Biol. 146, 185–201.

Piggee, C., 2008. Therapeutic antibodies coming through the pipeline. Anal. Chem. 80, 2305–2310.

Raison, R.L., Boux, H.A., 1985. Conformation dependence of a monoclonal antibody defined epitope on free human kappa chains. Mol. Immunol. 22, 1393–1398.

Ramsland, P., Brock, C., Moses, J., Robinson, B., Edmundson, A., Raison, R., 1999. Structural aspects of human IgM antibodies expressed in chronic B lymphocytic leukemia. Immunotechnology 4, 217–229.

Ramsland, P., Guddat, L., Edmundson, A., Raison, R., 1997. Diverse binding site structures revealed in homology models of polyreactive immunoglobulins. J. Comput. Aided Mol. Des. 11, 453–461.

Ramsland, P., Kaushik, A., Marchalonis, J., Edmundson, A., 2001. Incorporation of long CDR3s into V domains: implications for the structural evolution of the antibody-combining site. Exp. Clin. Immunogenet. 18, 176–198.

Sali, A., Blundell, T.L., 1993. Comparative protein modelling by satisfaction of spatial restraints. J. Mol. Biol. 234, 779–815.

Saul, F., Alzari, P., 1996. Crystallographic studies of antigen–antibody interactions. Methods Mol. Biol. 66, 11–23.

Schiffer, M., Girling, R., Ely, K., Edmundson, A., 1973. Structure of a lambda-type Bence–Jones protein at 3.5-A resolution. Biochemistry 12, 4620–4631.

Schueler-Furman, O., Wang, C., Baker, D., 2005. Progress in protein–protein docking: atomic resolution predictions in the CAPRI experiment using RosettaDock with an improved treatment of side-chain flexibility. Proteins 60, 187–194.

Terzyan, S., Bourne, C., Ramsland, P., Bourne, P., Edmundson, A., 2003. Comparison of the three-dimensional structures of a human Bence–Jones dimer crystallized on Earth and aboard US Space Shuttle Mission STS-95. J. Mol. Recognit. 16, 83–90.

Walker, K.Z., Boux, H.A., Hayden, G.E., Goodnow, C.C., Raison, R.L., 1985. A monoclonal antibody with selectivity for human kappa myeloma and lymphoma cells which has potential as a therapeutic agent. Adv. Exp. Med. Biol. 186, 833–841.